Energy 213 (2020) 118488

Contents lists available at ScienceDirect

Energy

journal homepage: www.elsevier.com/locate/energy

Hierarchical duality-based planning of transmission networks coordinating active distribution network operation

Jia Liu [a, b], Peter Pingliang Zeng [a, *], Hao Xing [a], Yalou Li [c], Qiuwei Wu [d]

[a] Department of Automation, Hangzhou Dianzi University, Hangzhou, 310018, China
[b] Department of Electrical Engineering, Zhejiang University, Hangzhou, 310027, China
[c] China Electric Power Research Institute, Beijing, 100192, China
[d] Center for Electric Power and Energy (CEE), Department of Electrical Engineering, Technical University of Denmark, Kongens Lyngby, 2800, Denmark

ARTICLE INFO

Article history:
Received 24 February 2020
Received in revised form
8 June 2020
Accepted 25 July 2020
Available online 8 August 2020

Keywords:
Transmission expansion
Active distribution network
Coordinated decision-making
Hierarchical optimization
Duality-based approach

ABSTRACT

The active distribution network becomes more stochastic due to high penetration of renewable energy sources, and it can transfer surplus power for transmission needs. If the distribution optimization problem collaborates with the conventional transmission expansion formulation, the coordination can also postpone the investment decisions for the transmission network, not only optimize the operation of the entire power system. In view of these, this paper presents a bi-level hierarchy transmission expansion formulation coordinating distribution networks. The upper level of the hierarchical decision-making framework corresponds to the objective and constraints of the transmission network, whereas the lower level relates to the distribution perspective. An approximation technique is used to make the constraints of the distribution network linear, which guarantees that the proposed bi-level program can be solved using the duality-based approach. Numerical tests carried out on two transmission-distribution integration networks demonstrate the effectiveness and high performance of the proposed hierarchical duality-based model to accommodate renewable energy. In addition, sensitivities of the transmission investment decisions are analysed in terms of externalities in transmission and distribution networks. Compared with conventional isolated optimization, results show that the total costs of T24D9 and T38D3 by the proposed hierarchical coordinated optimization can respectively reduce by 34.38 M$ and 382.23 M$. So the economic benefits are remarkable, and the proposed optimization is reasonable and valuable.

1. Introduction

With large-scale wind power resources penetrated, some challenges have arisen in the transmission networks, e.g. line congestion, voltage violation and wind power generation curtailment [1]. Since the network reinforcement is an effective approach to overcome these problems, the existing isolated expansion methodologies are notoriously costly. When the line investments are limited, the planning solution may not exist if the current isolated planning manner is applied to future integrated networks that include both transmission and distribution networks. On the other hand, integration of renewable energy sources [2] and demand response programs applications [3] in distribution level has led to change in the characteristics of restructured power systems, and uncertainties related to load variation should be considered appropriately [4]. Not only the variable output power of renewable distributed generators (DGs) highly depends on weather conditions [5], but also the aggregators of demand response and DGs could significantly impact the net load profiles of distribution networks [6]. As a result, the distribution networks can be regarded as dispatchable sources due to the available controls exploited [7], which could have great influences on the planning of transmission network. The power system planner can harvest additional flexibility by enabling interactions between transmission and distribution networks, which traditionally have been operated separately. Coordination between transmission and distribution networks can improve the operational economy of the entire power system and accommodate more DGs [8]. Thus, an integrated framework to determine the transmission expansion considering a coordinated operation with the distribution network is necessary

* Corresponding author.
E-mail address: pingliangzeng@126.com (P.P. Zeng).

https://doi.org/10.1016/j.energy.2020.118488
0360-5442/

Nomenclature

Sets and indices

$\Omega_{0/C}$	set of existing/alternative lines
Ω_I	set of buses
Ω_G (Ω_G^i)	set of conventional generators (connected to bus i)
Ω_{DG} (Ω_{DG}^i)	set of distributed generators (connected to bus i)
Ω_B	set of boundary buses between transmission and distribution networks
Ω_S	set of scenarios
Ξ_{UL}	set of upper-level decision variables
$\Xi_{PLL/DLL}$	set of primal/dual lower-level decision variables
$r(ij)$	$o(ij)$ indices of the receiving and origin buses of line ij

Continuous variables

$P_{g,s}^G$	power output of conventional generator g in scenario s
$P_{g,s}^{DG}$	power output of distributed generator g in scenario s
$P_{ij,s}$	power flow of line ij in scenario s
$P_{ij,s}^{loss}$	power loss of line ij in scenario s
$P_{i,s}^{T/D}$	power transmission/distribution network offers at boundary bus i in scenario s
$P_{i,s}^{RC}$	output curtailment of renewable energy at bus i in scenario s
$\theta_{i,s}$	voltage phase angle at bus i in scenario s

Dual continuous variables of primal constraints

$\alpha_{g,s}^{\max}$, $\alpha_{g,s}^{\min}$	dual variable associated with power output limits of distributed generators
$\delta_{ij,s}^{\max}$, $\delta_{ij,s}^{\min}$	dual variable associated with power flow limits of lines
$\psi_{i,s}^{\max}$, $\psi_{i,s}^{\min}$	dual variable associated with power flow limits between transmission and distribution networks at boundary buses
$C_{i,s}$	dual variable associated with power balance equation at buses
$\xi_{ij,s}$	dual variable associated with line power loss
$\gamma_{i,s}$	dual variable associated with output curtailment limit of renewable energy at buses

Binary variables

u_{ij}	binary variable for the construction of line ij
$u_{i,s}$	binary variable for the power flow direction at boundary bus i in scenario s

Parameters

C_{ij}	construction cost of line ij
$C_g^G(\cdot)$	cost function of conventional generator g
$C_g^{DG}(\cdot)$	cost function of distributed generator g
C_i^{RC}	curtailment cost of renewable energy per MWh at bus i
$\lambda_{i,s}^{T/D}$	energy price transmission/distribution network offers at boundary bus i in scenario s
$P_{ij}^{\max}$	upper power flow limit of line ij
$P_i^{\max}$	upper power flow limit between transmission and distribution networks at boundary bus i
$P_g^{G,\max}$ $P_g^{G,\min}$	upper and lower power output limits of conventional generator g
$P_{i,s}^{RF}$	output forecast of renewable energy at bus i in scenario s
$P_{i,s}^{L}$	load demand at bus i in scenario s
P_{ij}^0, Q_{ij}^0, V_i^0	base points of line ij and bus i
η_{ij}	annual value factor of line ij
Ψ_{ij}	annual discount rate of line ij
Λ_{ij}	lifetime of line ij
R_{ij}	B_{ij} resistance and susceptance of line ij
D_s	number of hours in scenario s
M	large positive number

and presented in this paper.

Installing transmission lines for a single target year requires providing a trade-off between line congestions and investment costs, which incorporates not only the first-stage expansion problem but also the second-stage operation optimization. The investment model in Refs. [9] is suitable for a market environment, which determines a secure and economic reinforcement solution for a transmission network integrating numbers of lower-level pool trading markets. Reference [10] reveals that consumption-based carbon emission accounting can affect expansion optimization and it can be explicitly incorporated into the transmission network constraints to observe the equity performance. A joint mechanism between transmission expansion and pay-as-bid auctions is proven to minimize system total costs over representative time intervals [11]. All the above expansion models unanimously assume that the locations and capacities of generation resources have been determined in advance while planning transmission networks and neglect the coordination between networks and generations. Inspired by Ref. [9], reference [12] simulates the market-based transmission expansion with generation allocation, which presents a joint auction market and a capacity mechanism to offer incentives for the interactions between transmission and generation. CO_2 mitigation and spinning reserve requirements can also affect the coordinated planning solutions for transmission and generation, and should be fully considered into the optimization framework [13]. Apart from stochastic optimization approach, reference [14] presents a robust expansion model for transmission network, which takes uncertainties of renewable energy generation and load variation into account. A robust decision-making framework in Ref. [15] is further formulated to exploit the additional flexibility of the integrated transmission and generation planning by implicating uncertain generation investment and retirement. Reference [16] further comprises the system outages and post-contingency corrective controls, and presents a co-optimization formulation under generation investment uncertainty in a min-max regret manner. Similar to conventional generators, investments in energy storage are co-optimized with transmission expansion to harvest significant revenue [17], and regulation decisions of loads are incorporated into the coordinated planning mechanism [18]. Reference [19] proposes to include the various network contingencies incorporating transmission expansion under load and wind power uncertainties. A stochastic generation and transmission expansion method with reliability criteria constrained is presented in Ref. [20], and a linearized

approximation method is then introduced. In effect, however, it is anticipated to mention the importance of tackling distribution network operation on the congestion levels of transmission networks. Thus, since the co-optimization of lower-level distribution network operation is ignored, all the above models could reduce or eliminate the revenue of transmission expansion.

The coordinated mechanism between transmission and distribution networks has been previously reported in the restructured environment, which primarily focuses on the power flow [21], the economic dispatch [22], the unit commitment [23], the expansion planning [24], the contingency analysis [25] and the flexibility estimation [26]. Reference [21] first investigates the distributed power flow method and master-slave-splitting solution technique to conduct a joint analysis for a transmission network integrating a number of distribution networks. In Ref. [22], a heterogeneous decomposition algorithm is presented to solve the coordinated optimal dispatch problem for integrated transmission and distribution networks, where the locational marginal prices (LMPs) and active power are interacted between the transmission system operator (TSO) and distribution system operators (DSOs). Different from Ref. [22], an improved multi-parametric quadratic programming (MPQP) [27] is developed to handle the transmission-distribution decentralized dispatch model. Reference [23] primarily formulates the transmission unit commitment relative to distribution networks in a system of systems based manner. The coordinated formulation in Ref. [28] is improved from Ref. [23] by encompassing the stochastic characteristics of system operation. Reference [24] proposes a decentralized decision-making framework to determine the robust transmission expansion and stochastic distribution expansion, which models the transmission wind uncertainty and distribution load uncertainty using uncertainty sets and numerical scenarios, respectively.

To handle this coordination, two methods have been studied, which comprise: the centralized optimization and the hierarchical optimization [29]. The centralized optimization may not be applied in practice because it can encounter some practical problems for modern power systems: 1) The transmission and distribution networks are supervised by the TSO and DSOs, respectively. Thus, it is difficult to observe the generation-network-load data of the current transmission and distribution networks in a unified manner. 2) The TSO and DSOs only share limited amounts of information at the boundary buses. This further prevents all independent networks in the centralized decision-making architecture from communicating with each other. 3) The problem size for optimizing the centralized power systems is so huge that both the solution efficiency and accuracy cannot be guaranteed. However, to address these drawbacks, the hierarchical optimization method can serve as a potential way to solve the coordination between transmission and distribution networks.

The hierarchical algorithms mentioned above can be generally classified into three groups: the Lagrangian relaxation [30], the optimality condition decomposition [31] and the heterogeneous decomposition [32]. Reference [33] preliminarily formulates the multi-area optimal power flow problem using the conventional Lagrangian relaxation, which integrates the Lagrangian function into the optimization objective of each regional network to satisfy the consistency demand for the boundary variables. The augmented Lagrangian relaxation in Ref. [34] improves the convergence properties of the iteration due to an additional quadratic term, which includes the auxiliary problem principle [29], the alternating direction method of multipliers [29] and the analytical target cascading [23]. Even though the convergence rate of the Lagrangian relaxation has been evolved from the augmented method, the algorithms still comprise an inconvenient parameter tuning procedure [35]. The optimality condition decomposition primarily includes the Karush-Kuhn-Tucker (KKT) decomposition [31], the Benders decomposition [36] and the MPQP [27]. In general, the advantages of the MPQP algorithm are the high convergence speed and a large application scale. However, the interactions between transmission and distribution networks are heterogeneous, that is, the boundary variables exchanged between the subsystems have different components. To be specific, the TSO sends the LMPs at the boundary buses to the DSOs while the DSOs send the boundary power injections to the TSO [22]. Thus, the heterogeneous decomposition explained in Ref. [32] is compatible with the hierarchical optimization of transmission and distribution networks, but it may encounter some convergence problems for the non-convex models.

The review of the above-mentioned studies reveals that, so far, the coordination mechanism between transmission and distribution networks has not been fully illustrated in the planning problem, i.e., the information of TSO-DSO interaction is heterogeneous rather than homogeneous in Ref. [24]. Moreover, uncertainties related to renewable energy generation and load variation in transmission and distribution networks have not been properly considered, e.g., renewable energy uncertainty in distribution network and renewable energy curtailment in transmission network are not investigated in Refs. [24]. Furthermore, the hierarchical algorithm to solve the transmission and distribution expansion problem still requires a time-consuming iteration process, i.e., the solution strategy in Refs. [24] only has linear convergence properties.

To address the above three issues, this paper proposes a bi-level hierarchy framework to optimize the transmission expansion in the presence of the coordinated operation of transmission and distribution networks. Different from the isolated transmission expansion [14], the bi-level formulation can account for detail topology of the distribution network and provide additional flexibility by deploying the TSO-DSO coordination. From the transmission's perspective, the TSO invests in transmission lines, dispatches the hourly generation schedule and sends the LMPs to the DSOs at the boundary buses. From the distribution's perspective, the DSOs operate a radial distribution network with renewable energy and deliver the boundary power injections to the TSO. It also enhances the performance of the transmission expansion for postponing the upgrades and reducing the investments. In the bi-level framework, the constraints of the upper-level transmission problem are modelled via the lossless dc approximation, and the lower-level distribution constraints are formulated using the linearized ac power flow model. The strong duality condition invoked between the primal and dual lower-level problems guarantees convergence and optimality of the equivalent model. The contributions of this paper comprise:

1) A bi-level stochastic formulation is developed to co-optimize the transmission expansion in the upper-level problem and distribution operation in the lower-level perspective. Uncertainties associated with renewable energy and loads in transmission and distribution networks are also properly considered.
2) The heterogeneous characteristics of TSO-DSO interaction are fully illustrated in this coordinated planning problem. To efficiently solve the original bi-level hierarchy, it is converted into a mixed-integer linear programming (MILP) single-level equivalent using the duality-based approach.
3) The resulting MILP model is computationally bearable with off-the-shelf solvers and is tested on two integrated systems, including T24D9 and T38D3.

2. Formulation of the bi-level hierarchy problem

The regular power system can be physically divided into the transmission network, distribution network and boundary network. The transmission network is managed by the TSO while the distribution network is in the charge of the DSO. The interactions between transmission and distribution networks create at the boundary, and the boundary bus in this paper defines as the root bus of a distribution network connected to the transmission network. The coordination mechanism between transmission and distribution networks is a process of multiple iterations. Interaction between distribution networks and the transmission network is achieved mainly through communication among TSO and DSOs. Hourly generation schedule is carried out and LMP is determined by TSO based on bid volumes offered by DSOs. According to LMP provided by TSO, each DSO optimizes the dispatch of DGs and redeclares the electricity bid volume to the TSO. By repeated information exchanges of LMP and bid volumes between transmission and distribution sides, a coordination equilibrium is achieved ultimately. It is worthy to mention that each DSO can both sell and purchase electricity in the bilateral market, i.e., the power exchange between transmission and distribution networks can be bi-directional in this paper.

Inspired by the autonomously cascaded nature of each independent network, the transmission planning coordinating distribution networks can be decomposed into two levels, and the proposed bi-level hierarchy problem is illustrated in Fig. 1. The upper-level problem aims to optimize the TSO investment and transmission generator schedule and formulates transmission operational constraints using a dc power flow model. The lower-level problem aims to optimize the DG schedule and renewable energy accommodation and formulates distribution operational constraints using the linearized ac power flow model in Ref. [37]. The TSO delivers the LMP ($\lambda_{i,s}$) to each DSO. In return, the DSO participates in the wholesale electricity market supervised by the TSO by sending transmission's ($C^T_{i,s}$,$P^T_{i,s}$) or distribution's ($C^D_{i,s}$,$P^D_{i,s}$) offers to sell electricity. To describe stochastic operation characteristics associated with the load and renewable (e.g., wind and hydropower [38]) generation feed-in, the scenario-based technique is used to describe different operating conditions and the optimization problem is modelled as a set of representative scenarios. The bi-level hierarchy problem is developed under the following formulation assumptions for different characteristics of the generators and network of the TSO and DSO:

1) The generation schedule for the transmission network is solely determined by the TSO, which optimizes its line construction solutions for a planning target year, while co-optimizing operations of transmission generators and wind power resources in each representative scenario. The lossless dc approximation is used in the transmission optimization problem, which has been accustomed to planning transmission networks as explained in Ref. [39]. Given that the use of the lossless dc formulation cannot take account of reactive power flows, the ac power flow with rectangular coordination can be applied to handle this problem. Although the reactive power flows could be better considered in the formulation presented to avoid any congestion in an actual network, especially in the wake of large renewable (e.g., wind and hydropower [40]) integration, the ac power flow based transmission expansion, as shown in Appendix A, coordinating distribution operation can be time-consuming. Besides, our simulations reveal that the lossless dc formulation has fairly high quality results while the computation time is much less than using the ac power flows. Thus, the lossless dc approximation is implemented in this paper to balance the solving accuracy and efficiency. The on/off status decisions of conventional generators in the transmission network are neglected in the upper-level problem to reduce the computational complexity and avoid handling non-convexities caused by binary variables. Although the minimum power outputs of the generators are not neglected in the upper-level problem, the practicability of the model is not severely limited, since the lower limits of power outputs of generators are very small. Our simulations show that this method would not lead to suboptimal solutions or even to unfeasible ones.
2) The DG schedule for the distribution network is separately dispatched by the DSO, which optimizes operations of DGs and renewable energy sources in each representative scenario. The distribution network studied in this paper is assumed to have the radial topology and the approximation in Ref. [27] is adopted to make the constraints of the distribution optimization problem linear. Although the use of the linearized ac network-loss model restricts our formulation to the radial distribution network, it can also be adapted to meshed distribution network in the presence of other power flow equations (e.g. LinDistFlow model [41]). Also, many fast DGs are assumed to be installed in the distribution network, and the constraints of ramping and spinning reserve can be ignored in the lower-level problem.
3) The DSO is interacted with the TSO at the single root bus. As the penetration of renewable energy sources in the distribution network increases, the DSO can sell surplus power to the TSO. The TSO and DSO should optimize their own autonomous network in the same operational scenarios.

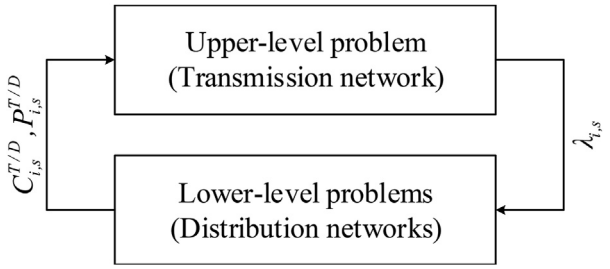

Fig. 1. Structure of bi-level hierarchy in coordinated transmission and distribution networks.

2.1. Upper-level problem

$$\min_{\Xi_{UL}} \sum_{ij\in\Omega_C} \eta_{ij} C_{ij} u_{ij} + \sum_{s\in\Omega_S} D_s \left[\sum_{g\in\Omega_G} C^G_g\left(P^G_{g,s}\right) + \sum_{i\in\Omega_B} C_{i,s}\left(P^D_{i,s} - P^T_{i,s}\right) + \sum_{i\in\Omega_I} C^{RC}_i P^{RC}_{i,s} \right] \tag{1}$$

$$\sum_{g\in\Omega^i_G} P^G_{g,s} - \sum_{ij\in\Omega_0} P_{ij,s} - \sum_{ij\in\Omega_C} P_{ij,s} + P^D_{i,s} - P^T_{i,s} + P^{RF}_{i,s} - P^{RC}_{i,s} = P^L_{i,s}, \forall i\in\Omega_I, s\in\Omega_S \tag{2}$$

$$P_{ij,s} = B_{ij}(\theta_{i,s} - \theta_{j,s}), \forall ij \in \Omega_0, s\in\Omega_S \tag{3}$$

$$\left|P_{ij,s}-B_{ij}\left(\theta_{i,s}-\theta_{j,s}\right)\right|\le M\left(1-u_{ij}\right),\ \forall ij\in\Omega_C,s\in\Omega_S \tag{4}$$

$$P_{ij,s}\le P_{ij}^{\max},\ \forall ij\in\Omega_0,s\in\Omega_S \tag{5}$$

$$P_{ij,s}\ge -P_{ij}^{\max},\ \forall ij\in\Omega_0,s\in\Omega_S \tag{6}$$

$$P_{ij,s}\le P_{ij}^{\max}u_{ij},\ \forall ij\in\Omega_C,s\in\Omega_S \tag{7}$$

$$P_{ij,s}\ge -P_{ij}^{\max}u_{ij},\ \forall ij\in\Omega_C,s\in\Omega_S \tag{8}$$

$$P_{g,s}^{G}\le P_{g}^{G,\max},\ \forall g\in\Omega_G,s\in\Omega_S \tag{9}$$

$$P_{g,s}^{G}\ge P_{g}^{G,\min},\ \forall g\in\Omega_G,s\in\Omega_S \tag{10}$$

$$P_{i,s}^{RC}\le P_{i,s}^{RF},\ \forall i\in\Omega_I,s\in\Omega_S \tag{11}$$

where $\Xi_{UL}=\{P_{g,s}^{G},P_{i,s}^{D},P_{i,s}^{T},P_{i,s}^{RC}\ge 0;u_{ij}\in\{0,\ 1\}P_{ij,s},\theta_{i,s}$:free$\}$. Equation (1) is to minimize the sum of investment and operation costs. Terms in (1) are, respectively, the line construction cost, the production cost of conventional generators, the energy cost distribution networks offer, and the curtailment cost of renewable energy. Note that $C_{i,s}$ in (1) is the dual variable of the nodal power balance constraint in the lower-level problem, which indicates the LMP at the boundary bus between transmission and distribution networks. Also, the quadratic cost function for conventional generators is used and linearized in the problem objective [42]. Parameter η_{ij} can be calculated using the net present value approach [43] as follows:

$$\eta_{\mathrm{ij}}=\frac{\Psi_{ij}\left(1+\Psi_{ij}\right)^{\Lambda_{ij}}}{\left(1+\Psi_{ij}\right)^{\Lambda_{ij}}-1} \tag{12}$$

Equation (2) enforces the nodal power balance for the transmission network. The branch flow equations in (3)-(4) are presented using the dc power flow model where the former is modelled for existing lines while the latter is formulated for alternative lines. Equations (5) and (6) constrain the power flow in existing transmission lines and (7)–(8) limit the power flow in alternative transmission lines. Equations 9 and 10 enforce limits on output of conventional generators. Equation (11) relates the output curtailment of renewable energy. Although large amounts of renewable energy curtailment may exist at the beginning of the iterations, the final solution of the formulated problem only has little or even no renewable energy curtailment. This is because the curtailment cost of renewable energy is relatively high. According to the equal incremental principle, renewable energy has a higher priority in the trade-off between conventional generators and renewable energy. Therefore, the minimum renewable energy curtailment can be achieved in this model. Our simulations indicate that this method is more efficient to guarantee the feasibility of the formulated problem.

When security constraints are considered in the upper-level transmission expansion formulation, contingencies should be incorporated into the above model. Since guaranteeing system security under all possible contingencies is practically impossible, the critical contingency selection approach in Ref. [44] is used to generate the contingency set and formulate the security-constrained transmission expansion problem. For each iteration, a set of critical contingencies is first selected and then the security analysis is performed for all critical contingencies. The iteration terminates if no post-contingency security constraints are violated for each contingency; otherwise, a new iteration with a modified contingency set begins. The detailed security-constrained transmission expansion formulation with a critical contingency set is similar to (1)–(12), with the difference that for each contingency a new branch node incidence matrix is generated and the number of lines in the examined right of way is reduced by the number of contingencies.

2.2. Primal lower-level problem

For each distribution network in each scenario, the lower-level problem is formulated as follows.

$$\min_{\Xi_{PLL}}\ \sum_{g\in\Omega_{DG}}C_{g}^{DG}\left(P_{g,s}^{DG}\right)+\lambda_{i,s}^{T}P_{i,s}^{T}-\lambda_{i,s}^{D}P_{i,s}^{D}+\sum_{i\in\Omega_I}C_{i}^{RC}P_{i,s}^{RC} \tag{13}$$

$$P_{g,s}^{DG}\le P_{g}^{DG,\max}:\left(\alpha_{g,s}^{\max}\right),\ \forall g\in\Omega_{DG},s\in\Omega_S \tag{14}$$

$$P_{g,s}^{DG}\ge P_{g}^{DG,\min}:\left(\alpha_{g,s}^{\min}\right),\ \forall g\in\Omega_{DG},s\in\Omega_S \tag{15}$$

$$\begin{aligned}&\sum_{g\in\Omega_{DG}^{i}}P_{g,s}^{DG}+\sum_{ij|r(ij)=i}\left(P_{ij,s}-P_{ij,s}^{loss}\right)-\sum_{ij|o(ij)=i}P_{ij,s}+P_{i,s}^{T}-P_{i,s}^{D}\\&+P_{i,s}^{RF}-P_{i,s}^{RC}=P_{i,s}^{L}:\left(C_{i,s}\right),\ \forall i\in\Omega_I,s\in\Omega_S\end{aligned} \tag{16}$$

$$P_{ij,s}^{loss}=\frac{\left(P_{ij}^{0}\right)^{2}+2P_{ij}^{0}\left(P_{ij,s}-P_{ij}^{0}\right)+\left(Q_{ij}^{0}\right)^{2}}{\left(V_{i}^{0}\right)^{2}\times R_{ij}}:\left(\xi_{ij,s}\right),\quad \forall ij\in\Omega_0,s\in\Omega_S \tag{17}$$

$$P_{ij,s}\le P_{ij}^{\max}:\left(\delta_{ij,s}^{\max}\right),\ \forall ij\in\Omega_0,s\in\Omega_S \tag{18}$$

$$P_{ij,s}\ge -P_{ij}^{\max}:\left(\delta_{ij,s}^{\min}\right),\ \forall ij\in\Omega_0,s\in\Omega_S \tag{19}$$

$$P_{i,s}^{T}\le P_{i}^{\max}u_{i,s}:\left(\psi_{i,s}^{\max}\right),\ \forall i\in\Omega_B,s\in\Omega_S \tag{20}$$

$$P_{i,s}^{D}\le P_{i}^{\max}\left(1-u_{i,s}\right):\left(\psi_{i,s}^{\min}\right),\ \forall i\in\Omega_B,s\in\Omega_S \tag{21}$$

$$P_{i,s}^{RC}\le P_{i,s}^{RF}:\left(\gamma_{i,s}\right),\ \forall i\in\Omega_I,s\in\Omega_S \tag{22}$$

where $\Xi_{PLL}=\{P_{g,s}^{DG},P_{i,s}^{D},P_{i,s}^{T},P_{i,s}^{RC}\ge 0;\ P_{ij,s},P_{ij,s}^{loss}$:free$\}$. Equation (13) aims to minimize the operation cost for each distribution network in each scenario, including the production cost of dispatchable DGs, the energy cost the transmission network offers, and the curtailment cost of renewable energy. Similar to the upper-level problem, the quadratic cost function for dispatchable DGs is used and linearized in the problem objective. Equations (14)-(15) limit the output of dispatchable DGs. The power flow balance constraints considering network loss are formulated in (16)-(17) where (17) is the linearized line loss equation using a first-order Taylor series expansion around the base points P_{ij}^{0}, Q_{ij}^{0}, V_{i}^{0} as in Ref. [37]. Note that the base points are appropriately chosen when all DGs generate the average of the minimum and maximum available outputs. Equations (18)-(19) enforce limits on the power flow in distribution lines. Equations (20)-(21) constrain the power exchange between transmission and distribution networks at the boundary bus. The output curtailment of renewable energy is

enforced in (22). The dual variable of each lower-level constraint is presented in parentheses. Note that after solving the upper-level problem, the transmission LMPs $\lambda_{i,s}^{T}$ are obtained and sent to the DSOs. With transmission LMPs given, the lower-level problem is formulated. The distribution LMPs $\lambda_{i,s}^{D}$ are then calculated as in Ref. [45].

3. Duality-based solution technique

The bi-level hierarchy problem in Section 2 can be handled using the following Solution Algorithm or the duality-based approach. Since the primal lower-level problem in Section 2.2 is a MILP, duality theory outperforms the Solution Algorithm [46]. Therefore, the duality-based solution technique is used and given below.

Solution Algorithm

Iteration number $k = 1$
Initialize $C_{i,s}^{D}(k), P_{i,s}^{D}(k)$ for $\forall i \in \Omega_B, s \in \Omega_S$ WHILE $k <$ maximum iteration number
a) Solve the upper-level problem and send the obtained $\lambda_{i,s}^{T}(k)$ for $\forall i \in \Omega_B, s \in \Omega_S$ to all DSOs.
b) With the updated $\lambda_{i,s}^{T}(k)$, solve the lower-level problems and obtain $C_{i,s}^{D}(k+1), P_{i,s}^{D}(k+1)$.
c) IF $\left|C_{i,s}^{D}(k+1) - C_{i,s}^{D}(k)\right| < \varepsilon_1, \left|P_{i,s}^{D}(k+1) - P_{i,s}^{D}(k)\right| < \varepsilon_2$ for $\forall i \in \Omega_B, s \in \Omega_S$, THEN exit.
ELSE: $k = k+1$, and send $C_{i,s}^{D}(k+1), P_{i,s}^{D}(k+1)$ to the TSO.
END WHILE

The dual form of the primal lower-level problem in Section 2.2 is derived in Section 3.1. The original bi-level problem is transformed into a single-level equivalent in Section 3.3 using the strong duality condition in Section 3.2. The equivalent model is a MILP after linearization, which can be solved using off-the-shelf solvers.

3.1. Dual lower-level problem

The dual form of the primal lower-level problem in (13)-(22) can be seen as follows.

$$\max_{\Xi_{DLL}} \sum_{g\in\Omega_G}\left(\alpha_{g,s}^{\max}P_g^{DG,\max} + \alpha_{g,s}^{\min}P_g^{DG,\min}\right) + \sum_{ij\in\Omega_0}\left(\delta_{ij,s}^{\max}P_{ij}^{\max} - \delta_{ij,s}^{\min}P_{ij}^{\max}\right) + \sum_{i\in\Omega_B}\left(\psi_{i,s}^{\max}P_i^{\max}u_{i,s} + \psi_{i,s}^{\min}P_i^{\max}(1-u_{i,s})\right) + \sum_{i\in\Omega_l} C_{i,s}\left(P_{i,s}^{L} - P_{i,s}^{RF}\right) + \sum_{ij\in\Omega_0}\xi_{ij,s}\frac{\left(Q_{ij}^{0}\right)^2 - \left(P_{ij}^{0}\right)^2}{\left(V_i^{0}\right)^2 \times R_{ij}} + \sum_{i\in\Omega_l}\gamma_{i,s}P_{i,s}^{RF} \tag{23}$$

$$\alpha_{g,s}^{\max} + \alpha_{g,s}^{\min} + C_{i(g),s} \le C_g^{DG},\ \forall g \in \Omega_{DG}, s \in \Omega_S \tag{24}$$

$$\delta_{ij,s}^{\max} + \delta_{ij,s}^{\min} - \frac{2P_{ij}^{0}}{\left(V_i^{0}\right)^2 \times R_{ij}}\xi_{ij,s} + C_{r(ij),s} - C_{o(ij),s} = 0,\ \forall ij \in \Omega_0, s \in \Omega_S \tag{25}$$

$$\psi_{i,s}^{\max} + C_{i,s}^{T} \le \lambda_{i,s}^{T},\ \forall i \in \Omega_B, s \in \Omega_S \tag{26}$$

$$\psi_{i,s}^{\min} - C_{i,s}^{D} \le -\lambda_{i,s}^{D},\ \forall i \in \Omega_B, s \in \Omega_S \tag{27}$$

$$\xi_{ij,s} - C_{r(ij),s} = 0,\ \forall i \in \Omega_l, s \in \Omega_S \tag{28}$$

$$\gamma_{i,s} - C_{i,s} \le C_i^{RC},\ \forall i \in \Omega_l, s \in \Omega_S \tag{29}$$

where $\Xi_{DLL} = \{\alpha_{g,s}^{\max}, \delta_{ij,s}^{\max}, \psi_{i,s}^{\max}, \psi_{i,s}^{\min}, \gamma_{i,s} \le 0; \alpha_{g,s}^{\min}, \delta_{ij,s}^{\min} \ge 0; C_{i,s}, \xi_{ij,s}: \text{free}\}$.

3.2. Strong duality condition

The following equation can be drawn invoking the strong duality theorem on the primal and dual lower-level problems.

$$\sum_{g\in\Omega_{DG}} C_g^{DG}\left(P_{g,s}^{DG}\right) + \lambda_{i,s}^{T}P_{i,s}^{T} - \lambda_{i,s}^{D}P_{i,s}^{D} + \sum_{i\in\Omega_l} C_i^{RC}P_{i,s}^{RC} = \sum_{g\in\Omega_{DG}}\left(\alpha_{g,s}^{\max}P_g^{DG,\max} + \alpha_{g,s}^{\min}P_g^{DG,\min}\right) + \sum_{ij\in\Omega_0}\left(\delta_{ij,s}^{\max}P_{ij}^{\max} + \sum_{i\in\Omega_l}\gamma_{i,s}P_{i,s}^{RF} - \delta_{ij,s}^{\min}P_{ij}^{\max}\right) + \sum_{i\in\Omega_B}\left(\psi_{i,s}^{\max}P_i^{\max}u_{i,s} + \psi_{i,s}^{\min}P_i^{\max}(1-u_{i,s})\right) + \sum_{i\in\Omega_l} C_{i,s}\left(P_{i,s}^{L} - P_{i,s}^{RF}\right) + \sum_{ij\in\Omega_0}\xi_{ij,s}\frac{\left(Q_{ij}^{0}\right)^2 - \left(P_{ij}^{0}\right)^2}{\left(V_i^{0}\right)^2 \times R_{ij}} \tag{30}$$

3.3. Single-level equivalent

The single-level equivalent can be proposed replacing the primal lower-level problem in the bi-level hierarchy with its constraints in (14)-(22), constraints of the dual lower-level problem in (24)-(29), and strong duality condition in (30). Thus, the equivalent can be eventually formulated as follows.

Eq. (1) (31)

Eq. (2) – (11), (14) – (22), (24) – (30) (32)

It is worthy to mention that the products $C_{i,s}P^{D}_{i,s}$ and $C_{i,s}P^{T}_{i,s}$ in (1) as well as $\psi^{\max}_{i,s}u_{i,s}$ and $\psi^{\min}_{i,s}(1-u_{i,s})$ in (30) are nonlinear. Each nonlinearity can be linearized as explained in Appendix B.

4. Case studies

In this section, two tests (i.e., T24D9 and T38D3) are carried out to validate the effectiveness and performance of the proposed hierarchical duality-based planning method for transmission networks coordinating active distribution networks. All simulations are scripted in MATLAB [47] with Gurobi solver v8.1.0 and the base points are acquired from the MATPOWER calculation results.

This paper considers three different optimization methods for the transmission and distribution networks:

Case 1. Isolated optimization [39]. In this case, the planning problem for the transmission network in Section 2.1 and the operation problem for distribution networks in Section 2.2 are optimized, respectively. Specifically, first the problem for distribution networks is optimized and then the problem formulation of the transmission network is solved by fixing the values obtained from the distribution networks.

Case 2. Hierarchical coordinated optimization. In this case, the single-level equivalent in Section 3.3 is deployed.

Case 3. Centralized coordinated optimization. In this case, the original bi-level problem for the transmission and distribution networks in Section 2 is solved in a joint manner. The centralized optimization can achieve an optimal solution, but cannot be implemented in practice, since the transmission and distribution networks are monitored by different operators. Thus, optimization results from this case are only deployed to check the validity of Case 2.

First, the results of different cases are simulated on T24D9 for comparison. The sensitivity analyses to parameters (i.e., wind farm locations and wind penetration levels) in the transmission network and parameters (i.e., renewable energy penetration levels and power flow limits of the lines between the transmission and distribution networks) in the distribution networks are investigated. Then, the proposed hierarchical duality-based planning method is further tested on T38D3 (i.e., a practical transmission network with three IEEE 33-bus distribution networks). Different from T24D9, T38D3 has the characteristic of high renewable energy (i.e., wind and hydropower [48]) penetration. The simulation results are reported below.

4.1. Test A-T24D9

T24D9 is an integrated generation-transmission-substation-distribution-load system which can be used to test or compare methods for performance analysis of transmission-distribution interaction. The objective is to define an interconnected system to provide a basis for reporting on analysis methods for the ability of the DSO to engage in bi-directional interactions with the TSO. There are numbers of distribution networks in the test system, but only nine distribution networks have the active regulation performance, which are thus selected as the research objects in this case. The detailed structure of T24D9 is displayed in Fig. 2. In the test system, the root buses of nine IEEE 33-bus distribution networks are connected to a modified IEEE RTS 24-bus transmission network at transmission buses 1, 2, 3, 5, 6, 7, 10, 13 and 19, respectively. The transmission network consists of 10 conventional generators, 38 existing lines and 17 demand sides. The transmission buses 3, 10 and 19 allocate wind farms with the total installed capacity of

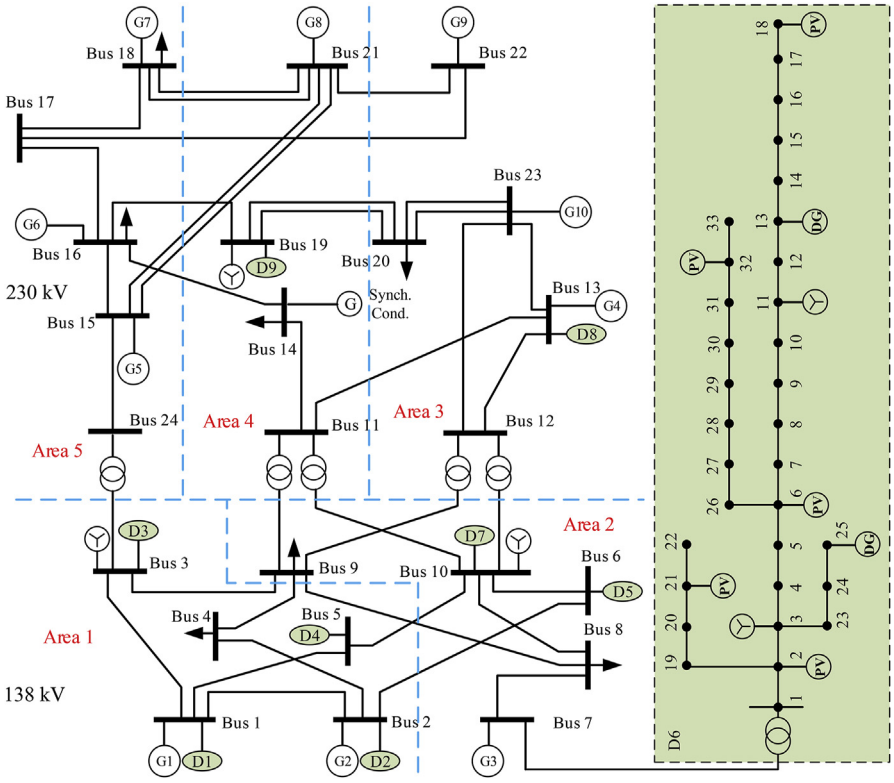

Fig. 2. Diagram of the original T24D9 system.

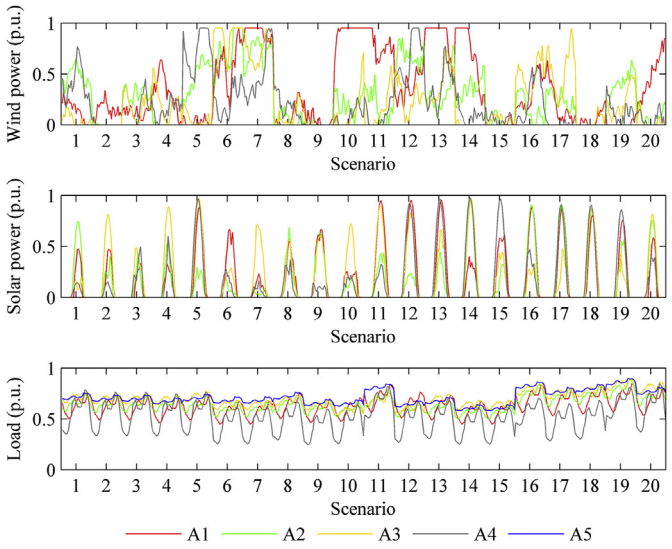

Fig. 3. Illustration of representative scenarios of renewable energy and loads in each area.

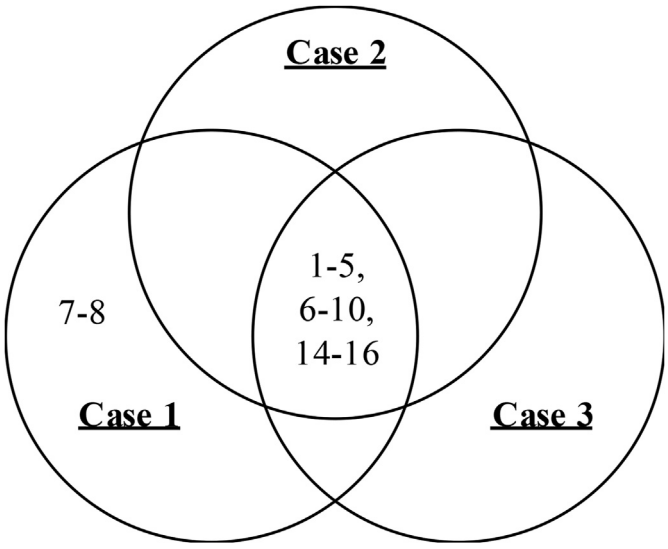

Fig. 4. Comparison of the transmission network planning solutions for different optimization methods.

300.0 MW. The nine distribution networks have the same topology, but the total demand, the locations of dispatchable DGs and the renewable energy (i.e., wind and photovoltaic) installation capacities are different. Take the distribution network 6 as an example, the total installed capacity of renewable energy is 34.22 MW and the load demand ranges between 30.23 and 72.25 MW. The test assumes the system can be divided into five areas. The yearly profiles of load demand and renewable generation in each area from historical data in Northwest China are reduced to 20 scenarios using the fuzzy C-means clustering approach in Ref. [49]. A matrix $A_{p\times q}$ that contains the 24 h of load data and renewable generation data for all of the days of the year creates the set of simulation data. p and q represent the number of days over a year, and load data and renewable generation data per day, respectively. Here, p equals 365 and q equals 72. After iterations, the synthesized clusters are used to represent all the samples in the original matrix. The representative scenarios to address the uncertainties associated with renewable energy and load variation are shown in Fig. 3. The index of representative scenarios and the number of days in the corresponding scenario are listed in Table 1. Compared with the original scenarios, the load factor and the renewable generation coefficient of each area keep almost constant after clustering. For example, the load factors of area 5 before and after scenario reduction are, respectively, 0.63 and 0.62. This indicates the high performance of the data clustering method. The upper limit of power exchange between transmission and distribution networks is set as 100 MW.

Table 1
Cluster results for each representative scenario.
1) Comparison of different optimization methods

Scenario	Index	No.	Scenario	Index	No.
1	2	10	11	178	24
2	8	36	12	210	5
3	15	10	13	253	10
4	39	14	14	258	17
5	65	17	15	265	20
6	97	18	16	283	12
7	118	9	17	285	19
8	138	24	18	303	28
9	139	26	19	318	35
10	154	18	20	365	13

This part compares the optimal transmission network expansion schemes for different optimization methods and their effects on the cost performance and renewable energy accommodation levels of the transmission and distribution networks. Also, the outputs of the conventional generators in the transmission network for different cases are investigated. Case 3 can achieve the global optimal planning solution for coordinated transmission and distribution networks. Fig. 4 shows the detail line reinforcement solutions under different cases. The optimal locations of transmission line reinforcement deemed in Case 2 and Case 3 are the same. This indicates the effectiveness of the proposed hierarchical coordinated optimization method. Additionally, it can be seen from Fig. 4 that, compared with Case 1, the number of locations with transmission lines constructed reduces in Case 2. This result indicates that coordination between transmission and distribution networks postpones the upgrades of the transmission network for the power exchange with distribution networks. In Case 2, one less transmission line is constructed between buses 7 and 8, which is close to the distribution network 6. This further indicates that the hierarchical coordinated optimization method contributes to the investment decrease of the transmission lines installed at the boundary buses between transmission and distribution networks.

Investing in transmission lines under different cases affects the cost performance and renewable energy accommodation in both transmission and distribution networks as listed in Table 2. In Case 2, the cost performance and renewable energy accommodation are consistently the same as those in Case 3. Thus, Case 2 yields the global optimal solutions for both transmission and distribution networks since Case 3 serves as a benchmark for the coordinated optimization results. As expected, Case 2 achieves smaller investment and generation costs for the integrated network than Case 1; however, note that the generation cost for distribution networks increases in Case 2. This phenomenon is mainly caused by flexible power exchange between transmission and distribution networks. Even though the distribution networks do not benefit from the coordination, the relative renewable energy accommodation share in the joint network in Case 2 is 1.27 times greater than that in Case 1 as the TSO and DSO also aim to use the coordination to decrease the renewable energy curtailment, not only to improve the cost performance.

Take scenario 14 as an example, the effects of different cases on

Table 2
Simulations results of different optimization methods.

Result		Case 1	Case 2	Case 3
Investment cost (M$)		2.76	2.29	2.29
Generation cost (M$)	Transmission	351.02	315.37	315.37
	Distribution	15.50	17.24	17.24
	Sum	366.52	332.61	332.61
Total cost (M$)		369.28	334.90	334.90
Renewable generation share (%)		5.59	7.11	7.11

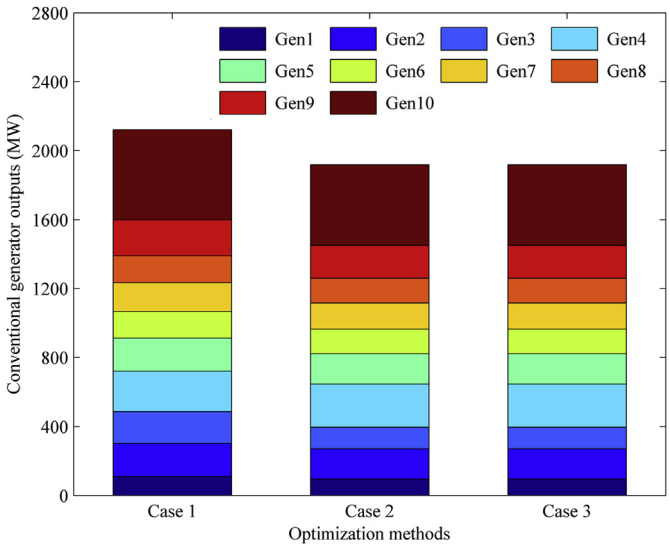

Fig. 5. Conventional generator outputs in the transmission network for different optimization methods in scenario 14.

the optimal conventional generator outputs in the transmission network are shown in Fig. 5. The expensive outputs of the transmission generators decrease in Case 2 since this case exploits the available control of distribution networks for the power exchange with the transmission network. Thus, Case 2 yields smaller transmission generation cost than Case 1. This reveals that the economic performance of the transmission operation benefits from the coordination between transmission and distribution networks.

As can be seen from Figs. 4 and 5, and Table 2, the effectiveness and high performance of the hierarchical coordinated optimization method are validated. Therefore, to further investigate the difference between the cost performance and conventional generator outputs in Case 1 and Case 2, the rest of the test considers these two cases only.

The reliability evaluation of the expansion schemes for Cases 1 (i.e., without TSO-DSO coordination) and 2 (i.e., with TSO-DSO coordination) is proposed at peak load. The formulation in Ref. [20] is used to assess the reliability of the planning solution for Case 1 while the formulation in Refs. [25] is implemented to evaluate the reliability of the expansion scheme for Case 2. Here, the loss of load probability (LOLP) is considered to cope with the reliability issue. The results show that the LOLP in Case 2 is zero, which indicates that load shedding is avoided with TSO-DSO interactions. However, the LOLP in Case 1 is 0.36, and the average load shedding with TSO-DSO coordination is 19.6 MW, which accounts for 0.9% of the total load. Thus, coordination between transmission and distribution networks can effectively reduce load curtailment, and the reliability of the network is also improved.

2) Sensitivity to parameters in the transmission network

This part simulates sensitivities of the transmission line investment decisions in the above part to the transmission network parameters. Here, the tested transmission network parameters include wind farm locations and wind penetration levels.

a) Effect of wind farm locations

To carry out this analysis, three different locations of the wind farms relative to distribution networks are considered; the wind power capacities installed in three different cases of wind farm locations are identical. The number of the distribution networks connected to the transmission buses with wind farms varies for each case. In location (3, 10, 19), the transmission buses with wind farms are all integrated with distribution networks; in location (3, 10, 14), the wind farms at transmission buses 3 and 10 are integrated with distribution networks; in location (9, 10, 14), the wind farm at transmission bus 10 is integrated with distribution network. As shown in Table 3 and Fig. 6, in Case 1, the transmission line decisions are related to wind farm locations. This is because the wind power profiles are stochastic and more line investment costs in the transmission network are needed at the buses with wind farms to reduce the transmission network congestion level. On the other hand, Case 2 yields the minimum transmission line investment cost if all the transmission buses with wind farms are connected with distribution networks since the available control in the

Table 3
Simulation results of different wind farm locations.

Result		Wind farm location					
		(3, 10, 19)[a]		(3, 10, 14)		(9, 10, 14)	
		Case 1	Case 2	Case 1	Case 2	Case 1	Case 2
Investment cost (M$)		2.76	2.29	4.03	3.47	4.82	3.55
Generation cost (M$)	Transmission	351.02	315.37	353.30	317.13	369.93	326.90
	Distribution	15.50	17.24	15.11	16.45	14.98	16.24
	Sum	366.52	332.61	368.41	333.58	384.91	343.14
Total cost (M$)		369.28	334.90	372.44	337.05	389.73	346.69
Renewable generation share (%)		5.59	7.11	5.03	6.39	4.89	6.21

[a] Indicates the corresponding case in Table 2.

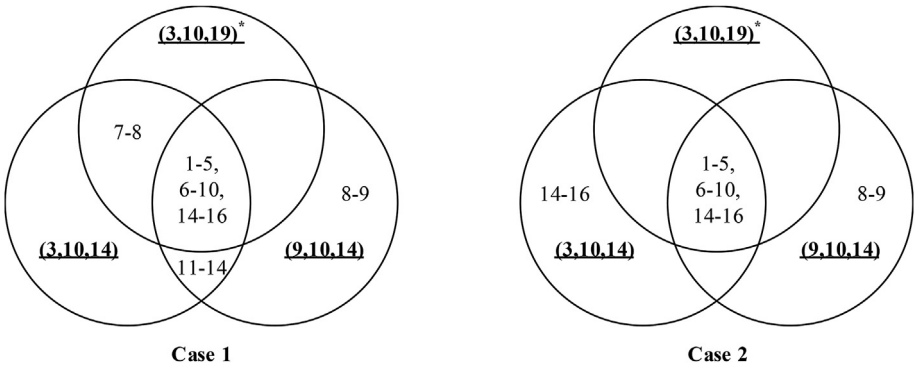

Fig. 6. Comparison of the transmission network planning solutions for different wind farm locations. * indicates the corresponding case in Fig. 3.

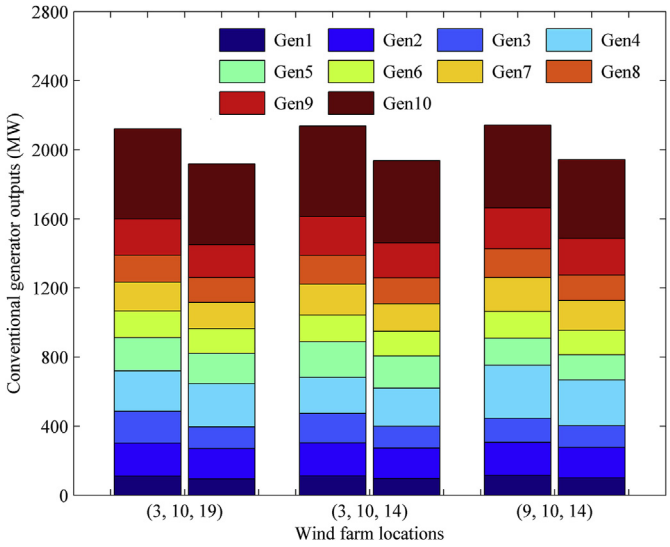

Fig. 7. Conventional generator outputs in the transmission network for different wind farm locations in scenario 14.

distribution network is exploited and the power injection at the boundary bus is more flexible to effectively guarantee the existing network security. Furthermore, compared with Case 1, the line investment cost in the transmission network reduces in Case 2 when the wind farms are located in the identical transmission buses. In both Case 1 and Case 2, the investment and generation costs associated with transmission line construction monotonically increase for further wind farms to distribution networks. It is worthy to mention that the renewable energy accommodation for the near locations of wind farms is greater than that for the remote locations of wind farms.

Fig. 7 compares the transmission generator outputs with different wind farm locations. In each wind farm location case, as in the previous part, Case 1 yields greater transmission generation cost than Case 2, resulting from the isolation between transmission and distribution networks. It is noteworthy that in both Case 1 and Case 2, the wind farm locations slightly affect the transmission generator outputs and thus the specific generation costs differ.

b) Effect of wind penetration levels

Since the wind penetration levels in the transmission network would affect the uncertainty of the bus injected power, it can change the transmission line investment decisions as illustrated in Fig. 8. As the wind penetration level increases, the number of transmission lines constructed does not reduce in both Case 1 and Case 2. Also, at the common wind penetration level, the transmission line investment decisions in Case 1 and Case 2 are different, which underlies the effect of the transmission-distribution coordination. Since the distribution networks in Case 1 are modelled as the constant loads connected to the boundary buses, it increases the demand for transmission line investments as the DSO cannot exploit any active management scheme for transmission needs. On the other hand, the model adopted in Case 1 is employed with loads that are regarded as constants. Different from the distribution networks represented in this model, Case 2 allows the DSO to receive more flexible power from the transmission network and thus it requires less transmission lines to reduce the transmission congestion at the identical wind penetration level. The cost performance and renewable energy accommodation level are summarized in Table 4. As expected, higher wind penetration levels lead to higher transmission line investments, lower generation costs and higher renewable generation shares, and Case 2 is consistently superior to Case 1.

Fig. 9 shows the transmission generator outputs with different wind penetration levels. The common thread for Case 1 and Case 2 is that as the wind penetration level increases, the outputs of conventional generators in the transmission network reduce. Furthermore, at each wind penetration level, the output rates in Case 1 and Case 2 vary for each transmission generator relative to the coordination optimization between transmission and distribution networks.

3) Sensitivity to parameters in the distribution network

Similar to the above part, this part further studies sensitivities of the transmission line investment decisions to the distribution network parameters. Also, the simulated distribution network parameters include renewable energy penetration levels and power flow limits of the lines between the transmission and distribution networks.

a) Effect of renewable energy penetration levels

Fig. 10 compares the transmission line investments for different renewable energy penetration levels in the distribution networks. In Case 2, the number of new transmission lines is the same for 50% and 100% penetrations levels of renewable energies, and only one additional line is built for the Case 150% penetration level of renewable energy. This is because of two factors: first, the DSO aims to minimize its operation cost by improving the renewable energy accommodation level in the distribution network and, second, the

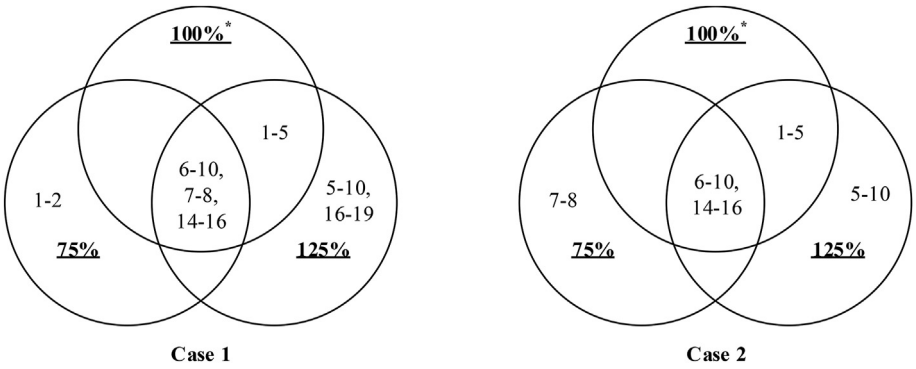

Fig. 8. Comparison of the transmission network planning solutions for different wind penetration levels. * indicates the corresponding case in Fig. 3.

Table 4
Simulation results of different penetration levels of renewable energy in the distribution networks.

Result		Renewable energy penetration level					
		50%		100%[a]		150%	
		Case 1	Case 2	Case 1	Case 2	Case 1	Case 2
Investment cost (M$)		2.58	2.12	2.76	2.29	2.85	2.38
Generation cost (M$)	Transmission	353.78	318.00	351.02	315.37	348.12	313.16
	Distribution	16.53	18.85	15.50	17.24	14.51	15.70
	Sum	370.31	336.85	366.52	332.61	362.63	328.86
Total cost (M$)		372.89	338.97	369.28	334.90	365.48	331.24
Renewable generation share (%)		5.22	5.82	5.59	7.11	6.31	8.02

[a] Indicates the corresponding case in Table 2.

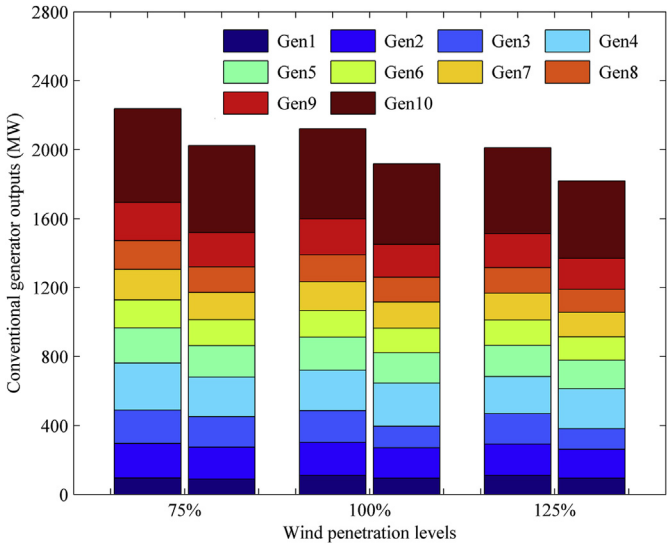

Fig. 9. Conventional generator outputs in the transmission network for different wind penetration levels in scenario 14. The left and right columns in each horizontal coordinate indicate Case 1 and Case 2, respectively.

DSO can manage renewable energy sources for arbitrage with the transmission network. As the renewable energy penetration level increases to 150%, so does the number of transmission lines constructed. In Case 1, where the DSO cannot evacuate surplus power from the root bus of the distribution network to the transmission network, the number of transmission lines constructed increases as the renewable energy penetration level increases.

Table 5 lists the simulation results with different renewable energy penetration levels. As in the previous part, Case 2 yields better cost performance and higher renewable energy accommodation than Case 1. Note that in Case 2, the renewable generation shares are more sensitive to the renewable energy penetration level than in Case 1.

The transmission generator outputs are compared in Fig. 11. In Case 2, the total transmission generator output reduces as the renewable energy penetration level increases. This result reveals that higher renewable energy penetration level in the distribution network prevents the use of conventional generators in the transmission network for the power balance of the entire power system, thus improving the value of the coordination between transmission and distribution networks.

b) Effect of the power flow limits of the lines between the transmission and distribution networks

Since the power exchange at the boundary bus between transmission and distribution networks can be limited, it can affect the behaviour of the DSO to participate in the arbitrage trading mechanism and thus alter the transmission line investments as shown in Fig. 12.

The number of new transmission lines in Case 1 is the same for 90% and 100% power flow limits of the lines between transmission and distribution networks, and only one additional line is built for the Case 110% power flow limit of the lines between transmission and distribution networks. This is because higher power flow limits allow the DSO to purchase more power from the transmission network, especially when the electricity price is low. As a result, as the power flow limit increases from 90% to 110%, the number of transmission lines constructed at the boundary buses increases. On the other hand, in Case 2, the number of new transmission lines for 90% power flow limit of the lines between transmission and distribution networks is two, which is only one new line less than 100% and 110% power flow limits of the lines between transmission

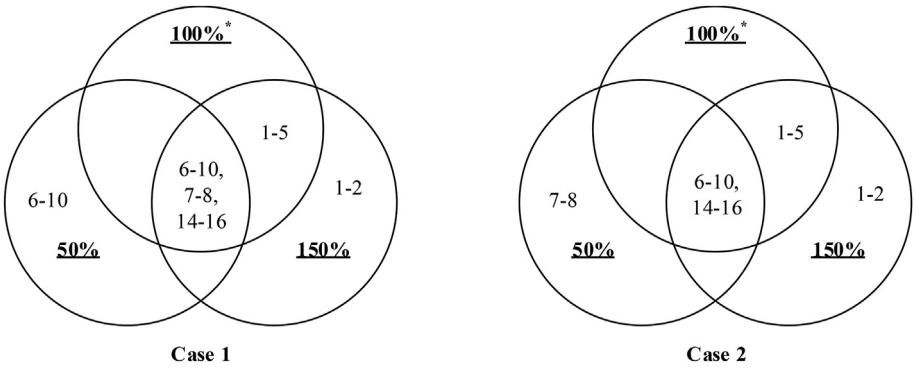

Fig. 10. Comparison of the transmission network planning solutions for different penetration levels of renewable energy in the distribution networks. * indicates the corresponding case in Fig. 3.

Table 5
Simulation results of different penetration levels of renewable energy in the distribution networks.

Result		Renewable energy penetration level					
		50%		100%[a]		150%	
		Case 1	Case 2	Case 1	Case 2	Case 1	Case 2
Investment cost (M$)		2.58	2.12	2.76	2.29	2.85	2.38
Generation cost (M$)	Transmission	353.78	318.00	351.02	315.37	348.12	313.16
	Distribution	16.53	18.85	15.50	17.24	14.51	15.70
	Sum	370.31	336.85	366.52	332.61	362.63	328.86
Total cost (M$)		372.89	338.97	369.28	334.90	365.48	331.24
Renewable generation share (%)		5.22	5.82	5.59	7.11	6.31	8.02

[a] Indicates the corresponding case in Table 2.

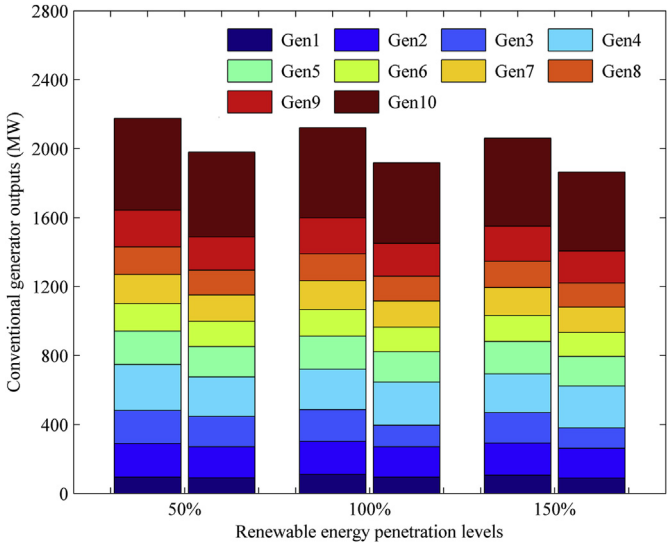

Fig. 11. Conventional generator outputs in the transmission network for different penetration levels of renewable energy in the distribution networks in scenario 14. The left and right columns in each horizontal coordinate indicate Case 1 and Case 2, respectively.

and distribution networks. Since more power can be transferred between transmission and distribution networks, the DSO aims to improve the renewable energy accommodation and cause greater power injection variation at the boundary buses. As a result, the number of transmission lines constructed near the distribution networks (buses 1 and 5) gradually increases.

The cost performance and renewable energy accommodation are compared in Table 6. The power flow limits can slightly affect the transmission line investments in the presence of the little change in the power flow limits of the lines between the transmission and distribution networks. Comparing the results for the cases 90%, 100% and 110% power flow limits, the total costs in both Case 1 and Case 2 increase as the power flow limit increases. This is because, with the increase of power flow limits, more power can be transferred between transmission and distribution networks and thus more transmission generators are dispatched, which results in increases in the production and total costs.

Fig. 13 illustrates the transmission generator outputs with different power flow limits. As in previous parts, the output of conventional generator 10 is greatest in the transmission network and Case 2 yields smaller total transmission generator output than Case 1. Interestingly, the power flow limit between transmission and distribution networks can slightly affect the total transmission generator output in Case 1, while there is a correlation in Case 2.

4) Sensitivity to ac and dc based models

This part investigates sensitivities of the transmission line investment decisions to different power flow models (i.e., ac and dc based models). The performance of the dc based transmission expansion coordinating linearized ac based distribution operation is validated and its results are compared with those of another method (i.e., ac based hierarchical coordinated optimization). A large-scale mixed integer non-linear programming formulation is obtained due to the non-convex characteristic of ac power flows, which introduces considerable challenges to the solving process. The results are shown in Table 7.

As the power flow models adopted change from dc formulation to ac one, the transmission investment costs reduce in all cases. From the viewpoint of generation costs, the results of dc based model are consistently smaller than those of ac based model, since

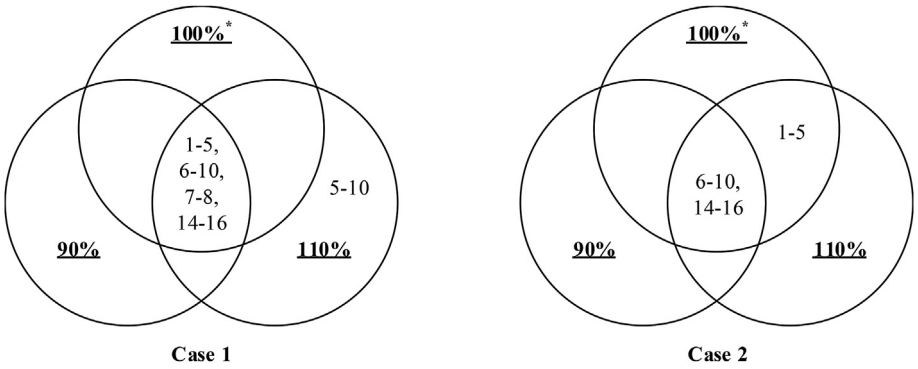

Fig. 12. Comparison of the transmission network planning solutions for different power flow limits of the lines between the transmission and distribution networks. * indicates the corresponding case in Fig. 3.

Table 6
Simulation results of different power flow limits of the lines between transmission and distribution networks.

Result		Power exchange limit					
		90%		100%[a]		110%	
		Case 1	Case 2	Case 1	Case 2	Case 1	Case 2
Investment cost (M$)		2.76	1.65	2.76	2.29	3.43	2.29
Generation cost (M$)	Transmission	347.96	307.87	351.02	315.37	352.30	317.57
	Distribution	17.01	19.13	15.50	17.24	15.11	16.45
	Sum	364.97	327.00	366.52	332.61	367.41	334.02
Total cost (M$)		367.73	328.65	369.28	334.90	370.84	336.31
Renewable generation share (%)		5.46	6.89	5.59	7.11	5.45	6.92

[a] Indicates the corresponding case in Table 2.

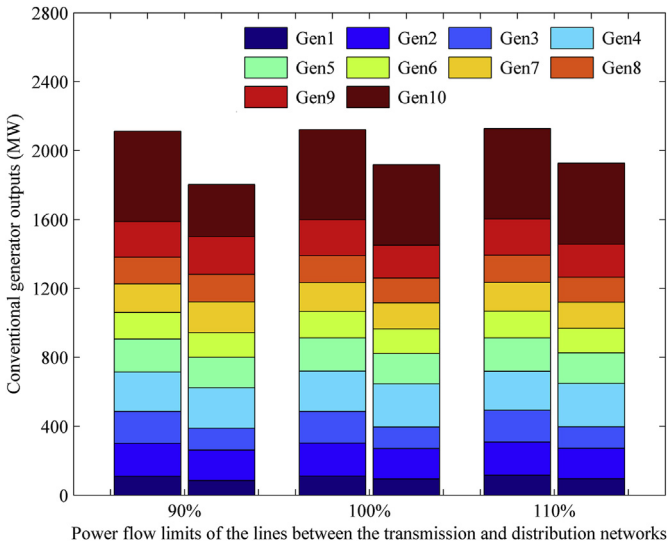

Fig. 13. Conventional generator outputs in the transmission network for different power flow limits of the lines between the transmission and distribution networks in scenario 14. The left and right columns in each horizontal coordinate indicate Case 1 and Case 2, respectively.

the reactive power flows in the network branches are considered in the ac network-loss formulation. The average difference between the total costs obtained by these two power flow models is 1.42% which is acceptable. However, the average computation time of ac based model is 16.4 times larger than that of dc based model which is very time-consuming. Although the dc based model could result in a slight decrease in total cost, it can be implemented in this paper to provide the trade-off between solving accuracy and efficiency.

4.2. Test B-T38D3

T38D3 is a typical-size integrated network, which is composed of five cascade provincial systems, i.e., Xinjiang, Gansu, Qinghai, Ningxia and Shaanxi. The power exchange between Xinjiang-Gansu, Gansu-Qinghai, Gansu-Ningxia and Gansu-Shaanxi can be two-way, i.e., one provincial power company can both sell and purchase electricity in the wholesale market. In addition, Xinjiang, Gansu, Qinghai, Ningxia and Shaanxi power grids constitute a regional network, which is a directly scheduled branch centre of the national electric power dispatching control centre. So, considering the area interconnection characteristic and power exchange performance, the proposed planning approach is further tested on T38D3. In this case, three IEEE 33-bus distribution networks are connected at buses 4, 10 and 20 of a practical 38-bus transmission network in Northwest China. Same as T24D9 in Section 4.1, the boundary buses for these distribution networks are all the root bus of each distribution network. The transmission network encompasses 55 conventional generators, 84 existing lines, 36 demand sides and 86 wind farms. The total installed capacity of wind resources is 490.5 GW. Transmission buses 2, 7, 17, 28, 29 and 31 host hydropower with the total installed capacity of 66 GW. Fig. 14 shows the diagram of the test system.

Fig. 15 depicts the total costs of transmission and distribution networks in T38D3 for different cases. It can be concluded that Case 2 achieves the same optimal solution as Case 3. This further indicates the validity of the hierarchical coordinated optimization method. Since Case 2 enables the coordination between transmission and distribution networks, it significantly reduces the overall total cost of T38D3.

Sensitivities of the transmission investment decisions to the capacity increase of hydropower are also studied. When the installed capacity of hydropower is increased to 125%, the total cost

Table 7
Simulation results of different power flow models.

Result		dc based model[a]			ac based model		
		Case 1	Case 2	Case 3	Case 1	Case 2	Case 3
Investment cost (M$)		2.76	2.29	2.29	2.46	2.13	2.13
Generation cost (M$)	Transmission	351.02	315.37	315.37	359.48	318.52	319.26
	Distribution	15.50	17.24	17.24	15.75	17.38	17.28
	Sum	366.52	332.61	332.61	375.23	335.90	336.54
Total cost (M$)		369.28	334.90	334.90	377.69	338.03	338.67
Computation time (sec.)		2.38	5.86	39.81	23.62	85.43	983.24

[a] Indicates the corresponding case in Table 2.

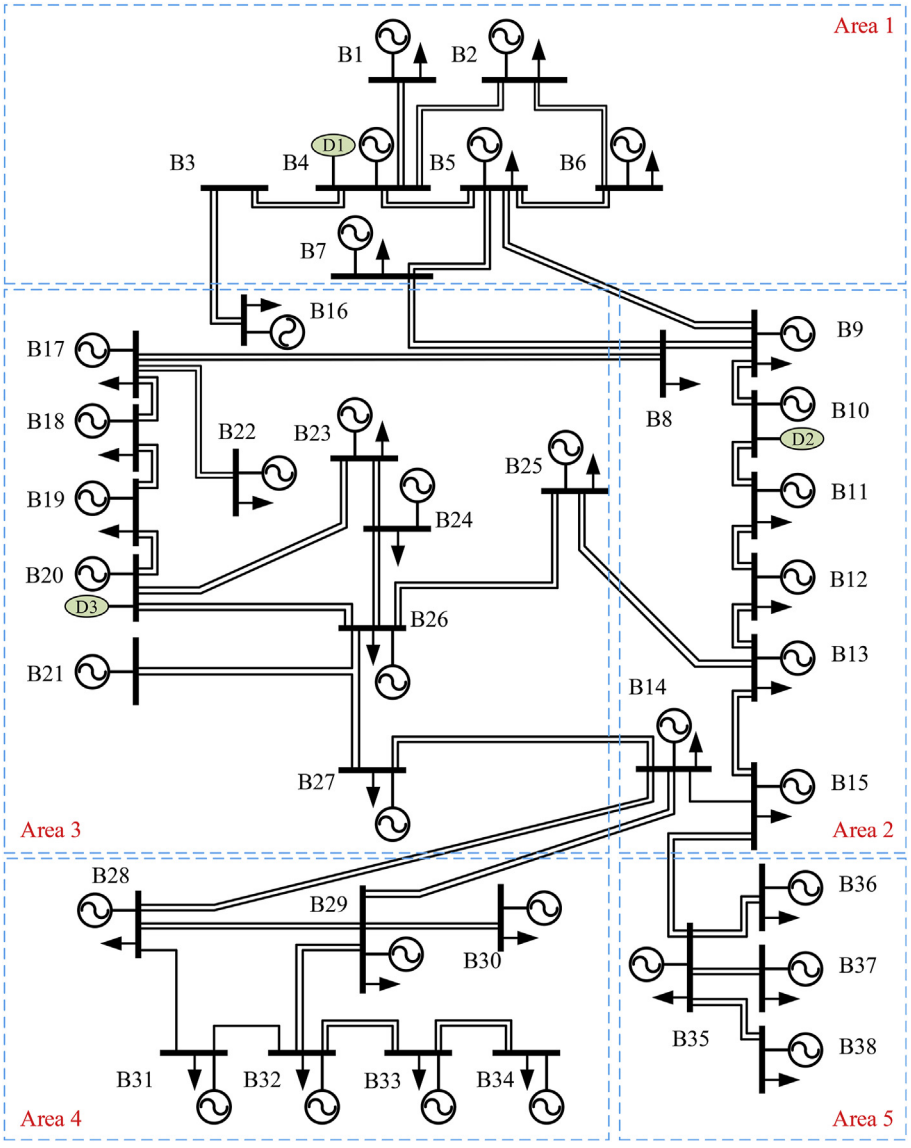

Fig. 14. Diagram of the original T38D3 system.

reduces by 4.09%, so the economic benefit is remarkable. In addition, the renewable generation share increases by 3.25%. However, when the installed capacity of hydropower is increased to 150%, no transmission planning solution can be achieved since there is no candidate transmission line to send the surplus power of hydropower to the demand side. This indicates that the increase of hydropower energy unlocks some economic and environmental benefits for the transmission expansion, but it can also bring some feasible challenges to the hierarchical coordinated optimization.

4.3. Convergence and optimality discussions

Simulations are carried out to study the computation performance of the hierarchical coordinated optimization. The

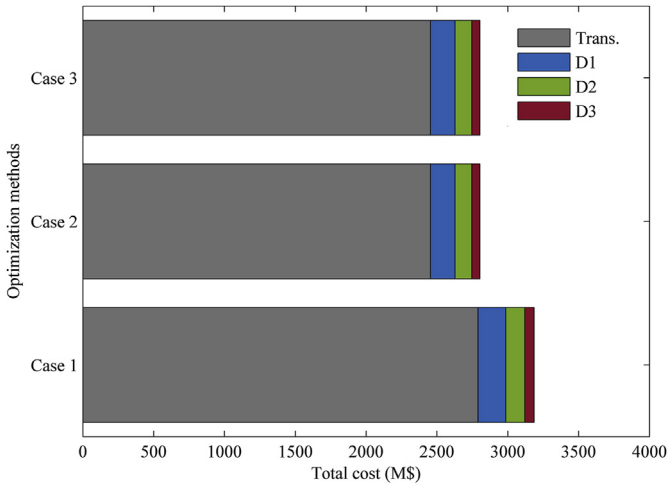

Fig. 15. Total cost of T38D3 for different optimization methods.

Table 8
Performance comparison of different cases.

Case	Comparison item	Gurobi v9.0	Hierarchical	Centralized
T24D9	Total cost (M$)	334.90	334.90	334.90
	Time (sec.)	4.69	5.86	39.81
T38D3	Total cost (M$)	2699.21	2686.86	2699.21
	Time (sec.)	9.75	12.51	260.24

hierarchical and centralized coordinated optimization computation performances for Cases T24D9 and T38D3 in terms of total costs and computation costs are compared in Table 8. The results of the centralized method, which are globally optimal, are served as the benchmark in Table 8. Moreover, since Gurobi v9.0 can tackle the bilinear problem directly, the computation performances are also investigated without the linearization of bilinear terms using the big-M method.

From the above table, it can be observed that the hierarchical coordinated optimization provides the best result for each of these cases, validating its high performance with respect to the optimality properties. The hierarchical coordinated optimization costs less computation time compared with the centralized coordinated optimization for all test systems, confirming its fast convergence features. The hierarchical coordinated optimization outperforms the centralized coordinated one in terms of the convergence speed. When implemented in a bigger power system (i.e., Case T38D3), the computation advantages of hierarchical coordinated optimization can be better unlocked, which justifies the robustness of the algorithm against the problem's scale. Furthermore, for two cases, Gurobi v9.0 can give the same total costs compared with the centralized coordinated optimization. This indicates that Gurobi v9.0 can find globally optimal solutions to bilinear problem. In terms of computation time, Gurobi v9.0 requires the least computation time, which delivers significant performance improvements since many more effective heuristic algorithms have been involved in this evolutionary version.

5. Conclusion

Coordinated transmission-distribution operation harvests additional flexibility to the restructured power systems with renewable energy source penetration. This coordination can reduce congestions of the existing transmission lines and thus postpone their upgrades. In this paper, a hierarchical modelling framework is proposed to optimize transmission investments, while co-optimizing the coordinated operation of transmission and distribution networks in a secure and economic manner. The bi-level formulation can not only account for different objectives of the TSO and DSOs, but also take into account their corresponding network constraints without exogenous equivalent simplifications. The interactions between transmission and distribution networks are heterogeneous: the TSO sends the LMPs at the boundary buses to the DSOs, and the DSOs deliver the boundary power injections to the TSO. To capture uncertainties associated with renewable energy and load variation, the optimization is performed over a set of representative scenarios. A MILP single-level equivalent is transformed from the original bi-level hierarchy using the duality-based approach, which is computationally bearable with off-the-shelf solvers.

The benefits of the hierarchical coordinated optimization are numerically validated on two integrated systems of different scales. The transmission-distribution coordination mechanism can benefit the transmission expansion, if the power exchange limits between transmission and distribution networks are sufficient. Also, the bi-level hierarchy has the same performance as the centralized optimization in reducing transmission investments and accommodating renewable energy. Sensitivities of the transmission investment decisions to externalities in the transmission and distribution networks are simultaneously investigated in the case studies. The transmission investments are sensitive to the renewable energy siting and sizing, and to the power transfer capability of the distribution network to interact with the transmission network.

The work presented in this paper points to the following future studies. First, the expansion model can be extended to handle dynamic programming scenario and incorporate distribution investment decisions. Second, the lower-level distribution operation problem can be improved in the presence of more active management schemes for distributed renewable energy and demand-side sources. Third, since contingencies and reliability measure are two important factors considered in transmission expansion, especially in the presence of large renewable integration, reliability could be better considered as a constraint in the proposed formulation, which would be reported in future studies.

CRediT authorship contribution statement

Jia Liu: Conceptualization, Methodology, Validation, Formal analysis, Data curation, Writing - original draft. **Peter Pingliang Zeng:** Conceptualization, Writing - original draft, Writing - review & editing, Supervision, Project administration, Funding acquisition. **Hao Xing:** Software, Data curation, Writing - original draft, Visualization. **Yalou Li:** Investigation, Writing - review & editing. **Qiuwei Wu:** Conceptualization, Resources, Writing - review & editing.

Declaration of competing interest

The authors declare that they have no known competing financial interests or personal relationships that could have appeared to influence the work reported in this paper.

Acknowledgments

This work was supported by the National Key R&D Program of China (grant no. 2018YFE0208400) and National Natural Science Foundation of China (grant no. U1766201). The authors are grateful to the editor and the anonymous reviewer for their insightful comments and suggestions.

Appendix A. Supplementary data

Supplementary data to this article can be found online at https://doi.org/10.1016/j.energy.2020.118488.

Appendix A. . AC based model

The ac power flow based transmission expansion formulation is given as follows.

$$\min_{\Xi_{UL}} \sum_{ij\in\Omega_C} \eta_{ij} C_{ij} u_{ij} + \sum_{s\in\Omega_S} D_s \left[\sum_{g\in\Omega_G} C_g^G \left(P_{g,s}^G\right) + \sum_{i\in\Omega_B} C_{i,s}\left(P_{i,s}^D - P_{i,s}^T\right) + \sum_{i\in\Omega_I} C_i^{RC} P_{i,s}^{RC} \right] \tag{A.1}$$

$$\sum_{g\in\Omega_G^i} P_{g,s}^G - \sum_{ij\in\Omega_0} P_{ij,s} - \sum_{ij\in\Omega_C} P_{ij,s} + P_{i,s}^D - P_{i,s}^T + P_{i,s}^{RF} - P_{i,s}^{RC} - G_i V_{i,s} = P_{i,s}^L, \forall i\in\Omega_I, s\in\Omega_S \tag{A.2}$$

$$\sum_{g\in\Omega_G^i} Q_{g,s}^G - \sum_{ij\in\Omega_0} Q_{ij,s} - \sum_{ij\in\Omega_C} Q_{ij,s} + B_i V_{i,s} = Q_{i,s}^L, \forall i\in\Omega_I, s\in\Omega_S \tag{A.3}$$

$$P_{ij,s} = -G_{ij} V_{i,s} + G_{ij} a_{ij,s} - B_{ij} b_{ij,s}, \forall ij\in\Omega_0, s\in\Omega_S \tag{A.4}$$

$$Q_{ij,s} = B_{ij} V_{i,s} - G_{ij} b_{ij,s} - B_{ij} a_{ij,s}, \forall ij\in\Omega_0, s\in\Omega_S \tag{A.5}$$

$$\left|P_{ij,s} + G_{ij} V_{i,s} - G_{ij} a_{ij,s} + B_{ij} b_{ij,s}\right| \le M(1-u_{ij}), \quad \forall ij\in\Omega_C, s\in\Omega_S \tag{A.6}$$

$$\left|Q_{ij,s} - \left(B_{ij} V_{i,s} - G_{ij} b_{ij,s} - B_{ij} a_{ij,s}\right)\right| \le M(1-u_{ij}), \quad \forall ij\in\Omega_C, s\in\Omega_S \tag{A.7}$$

$$a_{ij,s}^2 + b_{ij,s}^2 \le V_{i,s} V_{j,s}, \forall ij\in\Omega_0\cup\Omega_C, s\in\Omega_S \tag{A.8}$$

$$P_{ij,s}^2 + Q_{ij,s}^2 \le \left(S_{ij}^{\max}\right)^2, \forall ij\in\Omega_0, s\in\Omega_S \tag{A.9}$$

$$P_{ij,s}^2 + Q_{ij,s}^2 \le \left(S_{ij}^{\max}\right)^2 u_{ij}, \forall ij\in\Omega_C, s\in\Omega_S \tag{A.10}$$

$$V_{i,s} \le \left(U_i^{\max}\right)^2, \forall i\in\Omega_I, s\in\Omega_S \tag{A.11}$$

$$V_{i,s} \ge \left(U_i^{\min}\right)^2, \forall i\in\Omega_I, s\in\Omega_S \tag{A.12}$$

$$P_{g,s}^G \le P_g^{G,\max}, \forall g\in\Omega_G, s\in\Omega_S \tag{A.13}$$

$$Q_{g,s}^G \le Q_g^{G,\max}, \forall g\in\Omega_G, s\in\Omega_S \tag{A.14}$$

$$P_{g,s}^G \ge P_g^{G,\min}, \forall g\in\Omega_G, s\in\Omega_S \tag{A.15}$$

$$Q_{g,s}^G \ge Q_g^{G,\min}, \forall g\in\Omega_G, s\in\Omega_S \tag{A.16}$$

$$P_{i,s}^{RC} \le P_{i,s}^{RF}, \forall i\in\Omega_I, s\in\Omega_S \tag{A.17}$$

where $Q_{g,s}^G$ is the reactive power output of conventional generator g in scenario s, $Q_{ij,s}$ is the reactive power flow of line ij in scenario s, $Q_{i,s}^L$ is the reactive power demand at bus i in scenario s, $V_{i,s}$, $a_{ij,s}$ and $b_{ij,s}$ are the artificial variables introduced to transform the original non-convex ac based model into a convex one [50], G_i and B_i are, respectively, the shunt conductance and susceptance at bus i, G_{ij} is the conductance of line ij, $S_{ij}^{\max}$ is the maximum power flow of line ij, $U_i^{\max}$ and $U_i^{\min}$ are, respectively, the maximum and minimum voltage magnitude of bus i, $Q_g^{G,\max}$ and $Q_g^{G,\min}$ are the maximum and minimum reactive power output of conventional generator g, respectively.

Equations (A.2) and (A.3) enforce balance between nodal active and reactive power. Equations (A.4) and (A.5) are the active and reactive power flow constraints for existing lines, respectively, whereas (A.6) and (A.7) are, respectively, the active and reactive power flow constraints for alternative lines. Equation (A.8) relates the cone constraint. Equations (A.9) and (A.10) limit the apparent power flows in existing and alternative lines, respectively. Equations (A.11) and (A.12) constrain the bus voltage magnitude. Equations (A.13)-(A.16) represent the constraints of active and reactive power outputs of conventional generators. Note that the following constraints related to voltage phase angle variables could be incorporated into the above formulation to guarantee the exactness for mesh networks [51].

$$\theta_{j,s} - \theta_{i,s} = \mathrm{atan2}\left(b_{ij,s}, a_{ij,s}\right), \forall i,j\in\Omega_I, s\in\Omega_S \tag{A.18}$$

However, since (A.18) includes the non-convex terms, it can be time-consuming to handle this integrated formulation. To provide the trade-off between solving accuracy and efficiency, (A.18) can be relaxed in the ac based model, because the formulation of (A.1)-(A.17) is a strict relaxation for transmission networks. Reference [51] has investigated that the formulation without (A.18) has pretty high computational speed in the sacrifice of little quality compared with the best convex relaxation method of (A.18). Thus, the ac based model with (A.18) relaxed is applied in this paper to formulate the second order cone programming based transmission expansion.

Appendix B. Linearization

Products of continuous and binary variables can be linearized using the big-M method. For the multiplications of $\psi_{i,s}^{\max} u_{i,s}$ and $\psi_{i,s}^{\min}(1-u_{i,s})$ in (30), the product $\psi_{i,s}^{\max} u_{i,s}$ is denoted as $c_{i,s}$ and $\psi_{i,s}^{\min}(1-u_{i,s})$ is denoted as $n_{i,s}$. Then, the following linear equivalent of the original nonlinear problem can be obtained.

$$-M(1-u_{i,s}) \le c_{i,s} - \psi_{i,s}^{\max} \le M(1-u_{i,s}) \tag{B.1}$$

$$-Mu_{i,s} \le c_{i,s} \le Mu_{i,s} \tag{B.2}$$

$$-Mu_{i,s} \le n_{i,s} - \psi_{i,s}^{\min} \le Mu_{i,s} \tag{B.3}$$

$$-M(1-u_{i,s}) \le n_{i,s} \le M(1-u_{i,s}) \tag{B.4}$$

Note that the selection of parameter M is tricky, and its value can be selected using the appropriate technique in Ref. [52]. Empirically, large parameters can cause oscillations for the optimization problem, while small parameters may result in local optimality. In

this paper, M is set as 10000, and has been manually checked that it does not compromise the optimality.

Products of two continuous variables can be linearized using the big-M method and the KKT condition. For the products $C_{i,s}P^D_{i,s}$ and $C_{i,s}P^T_{i,s}$, the third term in (1), denoted below as K_e, can be rewritten as the following equation expressing $C_{i,s}$ from (26)-(27)

$$\begin{aligned} K_e &= \sum_{i\in\Omega_B} C_{i,s}\left(P^D_{i,s}-P^T_{i,s}\right) \\ &= \sum_{i\in\Omega_B}\left(\psi^{\min}_{i,s}P^D_{i,s}+\lambda^D_{i,s}P^D_{i,s}+\psi^{\max}_{i,s}P^T_{i,s}-\lambda^T_{i,s}P^T_{i,s}\right) \end{aligned} \tag{B.5}$$

Then, using the KKT conditions of (20)-(21), the above equation can be rearranged as

$$\begin{aligned} K_e = \sum_{i\in\Omega_B}\Big[&\psi^{\max}_{i,s}P^{\max}_i u_{i,s}+\psi^{\min}_{i,s}P^{\max}_i(1-u_{i,s}) \\ &+\lambda^D_{i,s}P^D_{i,s}-\lambda^T_{i,s}P^T_{i,s}\Big] \end{aligned} \tag{B.6}$$

The nonlinear multiplications of $\psi^{\max}_{i,s}u_{i,s}$ and $\psi^{\min}_{i,s}(1-u_{i,s})$ in (B.6) can be linearized using (B.1)-(B.4).

References

[1] Pfeifer A, Dobravec V, Pavlinek L, Krajačić G, Duić N. Integration of renewable energy and demand response technologies in interconnected energy systems. Energy Jul. 2018;161:447–55.
[2] Li K, Wang F, Mi Z, Fotuhi-Firuzabad M, Duić N, Wang T. Capacity and output power estimation approach of individual behind-the-meter distributed photovoltaic system for demand response baseline estimation. Appl Energy Jul. 2019;253:113595.
[3] Wang F, Xiang B, Li K, Ge X, Lu H, Lai J, et al. Smart households' aggregated capacity forecasting for load aggregators under incentive-based demand response programs. IEEE Trans Ind Appl Mar. 2020;56:1086–97.
[4] Lu X, Li K, Xu H, Wang F, Zhou Z, Zhang Y. Fundamentals and business model for resource aggregator of demand response in electricity markets. Energy Aug. 2020;204:117885.
[5] Zhen Z, Pang S, Wang F, Li K, Li Z, Ren H, et al. Pattern classification and PSO optimal weights based sky images cloud motion speed calculation method for solar PV power forecasting. IEEE Trans Ind Appl Jul. 2019;55:3331–42.
[6] Honarmand ME, Hosseinnezhad V, Ghazizadeh MS, Wang F, Siano P. A peak-load-reduction-based procedure to manage distribution network expansion by applying process-oriented costing of incoming components. Energy Jul. 2019;186:115852.
[7] Liu J, Cheng H, Zeng P, Yao L. Rapid assessment of maximum distributed generation output based on security distance for interconnected distribution networks. Int J Electr Power Energy Syst Mar. 2018;101:13–24.
[8] Hadush SY, Meeus L. DSO-TSO cooperation issues and solutions for distribution grid congestion management. Energy Pol Jun. 2018;120:610–21.
[9] Garces LP, Conejo AJ, Garcia-Bertrand R, Romero R. A bilevel approach to transmission expansion planning within a market environment. IEEE Trans Power Syst Aug. 2009;24:1513–22.
[10] Sun Y, Kang C, Xia Q, Chen Q, Zhang N, Cheng Y. Analysis of transmission expansion planning considering consumption-based carbon emission accounting. Appl Energy May 2017;193:232–42.
[11] Farrell N, Devine MT, Soroudi A. An auction framework to integrate dynamic transmission expansion planning and pay-as-bid wind connection auctions. Appl Energy Oct. 2018;228:2462–77.
[12] Roh JH, Shahidehpour M, Fu Y. Market-based coordination of transmission and generation capacity planning. IEEE Trans Power Syst Nov. 2007;22:1406–19.
[13] Guerra OJ, Tejada DA, Reklaitis GV. An optimization framework for the integrated planning of generation and transmission expansion in interconnected power systems. Appl Energy May 2016;170:1–21.
[14] Chatthaworn R, Chaitusaney S. Improving method of robust transmission network expansion planning considering intermittent renewable energy generation and loads. IET Gener, Transm Distrib Apr. 2015;9:1621–7.
[15] Chen B, Wang L. Robust transmission planning under uncertain generation investment and retirement. IEEE Trans Power Syst Nov. 2016;31:5144–52.
[16] Moreira A, Strbac G, Moreno R, Street A, Konstantelos I. A five-level MILP model for flexible transmission network planning under uncertainty: a min–max regret approach. IEEE Trans Power Syst Jan. 2018;33:486–501.
[17] Dvorkin Y, Fernandez-Blanco R, Wang Y, Xu B, Kirschen DS, Pandzic H, et al. Co-planning of investments in transmission and merchant energy storage. IEEE Trans Power Syst Jan. 2018;33:245–56.
[18] Zhang N, Hu Z, Shen B, Dang S, Zhang J, Zhou Y. A source–grid–load coordinated power planning model considering the integration of wind power generation. Appl Energy Apr. 2016;168:13–24.
[19] Orfanos GA, Georgilakis PS, Hatziargyriou ND. Transmission expansion planning of systems with increasing wind power integration. IEEE Trans Power Syst May 2013;28:1355–62.
[20] Aghaei J, Amjady N, Baharvandi A, Akbari M-A. Generation and transmission expansion planning: MILP–based probabilistic model. IEEE Trans Power Syst Jul. 2014;29:1592–601.
[21] Sun H, Guo Q, Zhang B, Guo Y, Li Z, Wang J. Master–slave-splitting based distributed global power flow method for integrated transmission and distribution analysis. IEEE Trans. Smart Grid May 2015;6:1484–92.
[22] Li Z, Guo Q, Sun H, Wang J. Coordinated economic dispatch of coupled transmission and distribution systems using heterogeneous decomposition. IEEE Trans Power Syst Nov. 2016;31:4817–30.
[23] Kargarian A, Fu Y. System of systems based security-constrained unit commitment incorporating active distribution grids. IEEE Trans Power Syst Sep. 2014;29:2489–98.
[24] Nikoobakht A, Aghaei J, Massrur HR, Hemmati R. Decentralised hybrid robust/stochastic expansion planning in coordinated transmission and active distribution networks for hosting large-scale wind energy. IET Gener, Transm Distrib Jan. 2020;14:797–807.
[25] Jia H, Qi W, Liu Z, Wang B, Zeng Y, Xu T. Hierarchical risk assessment of transmission system considering the influence of active distribution network. IEEE Trans Power Syst Mar. 2015;30:1084–93.
[26] Silva J, Sumaili J, Bessa RJ, Seca L, Matos MA, Miranda V, et al. Estimating the active and reactive power flexibility area at the TSO-DSO interface. IEEE Trans Power Syst Sep. 2018;33:4741–50.
[27] Lin C, Wu W, Chen X, Zheng W. Decentralized dynamic economic dispatch for integrated transmission and active distribution networks using multi-parametric programming. IEEE Trans. Smart Grid Sep. 2018;9:4983–93.
[28] Kargarian A, Fu Y, Wu H. Chance-constrained system of systems based operation of power systems. IEEE Trans Power Syst Sep. 2016;31:3404–13.
[29] Molzahn DK, Dorfler F, Sandberg H, Low SH, Chakrabarti S, Baldick R, et al. A survey of distributed optimization and control algorithms for electric power systems. IEEE Trans. Smart Grid Nov. 2017;8:2941–62.
[30] Qu K, Yu T, Huang L, Yang B, Zhang X. Decentralized optimal multi-energy flow of large-scale integrated energy systems in a carbon trading market. Energy Feb. 2018;149:779–91.
[31] Nogales FJ, Prieto FJ, Conejo AJ. A decomposition methodology applied to the multi-area optimal power flow problem. Ann Oper Res Apr. 2003;120:99–116.
[32] Zhao J, Zhang Z, Yao J, Yang S, Wang K. A distributed optimal reactive power flow for global transmission and distribution network. Int J Electr Power Energy Syst Jan. 2019;104:524–36.
[33] Conejo AJ, Aguado JA. Multi-area coordinated decentralized DC optimal power flow. IEEE Trans Power Syst Nov. 1998;13:1272–8.
[34] Xie M, Ji X, Hu X, Cheng P, Du Y, Liu M. Autonomous optimized economic dispatch of active distribution system with multi-microgrids. Energy Apr. 2018;153:479–89.
[35] Biskas PN, Bakirtzis AG. Decentralised OPF of large multiarea power systems. Proc. Inst. Elect. Eng., Gen., Transm., Distrib. Jan. 2006;153:99–105.
[36] Zhou H, Zheng JH, Li Z, Wu QH, Zhou XX. Multi-stage contingency-constrained co-planning for electricity-gas systems interconnected with gas-fired units and power-to-gas plants using iterative Benders decomposition. Energy May 2019;180:689–701.
[37] Zheng W, Wu W, Liu Y, Li Z, Zhang B. Fully distributed multi-area economic dispatch method for active distribution networks. IET Gener, Transm Distrib Sep. 2015;9:1341–51.
[38] Jiang Z, Li A, Ji C, Qin H, Yu S, Li Y. Research and application of key technologies in drawing energy storage operation chart by discriminant coefficient method. Energy Aug. 2016;114:774–86.
[39] MacRae CAG, Ernst AT, Ozlen M. A Benders decomposition approach to transmission expansion planning considering energy storage. Energy Aug. 2016;112:795–803.
[40] Jiang Z, Ji C, Qin H, Feng Z. Multi-stage progressive optimality algorithm and its application in energy storage operation chart optimization of cascade reservoirs. Energy Feb. 2018;148:309–23.
[41] Baran ME, Wu FF. Network reconfiguration in distribution systems for loss reduction and load balancing. IEEE Trans Power Deliv Apr. 1989;4:1401–7.
[42] Younes M, Khodja F, Kherfane RL. Multi-objective economic emission dispatch solution using hybrid FFA (firefly algorithm) and considering wind power penetration. Energy Jan. 2014;67:595–606.
[43] Liu J, Cheng H, Zeng P, Yao L, Shang C, Tian Y. Decentralized stochastic optimization based planning of integrated transmission and distribution networks with distributed generation penetration. Appl Energy Apr. 2018;220:800–13.
[44] Jabr RA. Homogeneous cutting-plane method to solve the security-constrained economic dispatching problem. IEE Proc Generat Transm Distrib Mar. 2002;149:139–44.
[45] Li R, Wu Q, Oren SS. Distribution locational marginal pricing for optimal electric vehicle charging management. IEEE Trans Power Syst Jan. 2014;29:203–11.
[46] Arroyo JM. Bilevel programming applied to power system vulnerability analysis under multiple contingencies. IET Gener, Transm Distrib Feb. 2010;4:

178–90.
[47] Liu J, Cheng H, Tian Y, Yao L. An optimal N-1 secure operation mode for medium voltage loop distribution networks considering load supply capability and security distance. Elec Power Compon Syst Nov. 2017;45:1393–403.
[48] Jiang Z, Li R, Li A, Ji C. Runoff forecast uncertainty considered load adjustment model of cascade hydropower stations and its application. Energy Jun. 2018;158:693–708.
[49] Liu J, Cheng H, Tian Y, Zeng P, Yao L. Multi-objective bi-level planning of active distribution networks considering network transfer capability and dispersed energy storage systems. J Renew Sustain Energy Jan. 2018;10:015501.
[50] Kocuk B, Dey SS, Sun XA. New formulation and strong MISOCP relaxations for AC optimal transmission switching problem. IEEE Trans Power Syst Nov. 2017;32:4161–70.
[51] Kocuk B, Dey SS, Sun XA. Strong SOCP relaxations for the optimal power flow problem. Oper Res Nov. 2016;64:1177–96.
[52] Soltysik RC, Yarnold PR. Two-group multioda: a mixed-integer linear programming solution with bounded m. Optim. Data Anal. Sep. 2010;1:30–7.